Microstructure near corners of continuous-cast steel slabs showing three-dimensional frozen meniscus and hooks

Go-Gi Lee [a], Brian G. Thomas [b,*], Ho-Jung Shin [c], Seung-Kwan Baek [d], Choon-Haeng Choi [d]
Dong-Su Kim [d], Sung-Jong Yu [d] and Seon-Hyo Kim [a]

[a] Department of Materials Science and Engineering, Pohang University of Science & Technology, South Korea
[b] Department of Mechanical Science and Engineering, University of Illinois at Urbana-Champaign, Illinois USA
[c] POSCO Technical Research Laboratories, Continuous Casting, POSCO, Gwangyang Works, South Korea
[d] POSCO Steelmaking Department, Technology Development Group, POSCO, Gwangyang Works, South Korea
[*] Corresponding author. Tel.: +1 217 333 6919; fax: +1 217 244 6534. *E-mail address:* bgthomas@uiuc.edu (B.G. Thomas)

ABSTRACT

Frozen meniscus features near the slab corners in continuous-cast ultra-low-carbon steel samples were investigated using special etching reagents and optical microscopy. The three-dimensional continuous shapes of hook defects along the oscillation marks around the slab corners were constructed from a set of micrographs taken at different vertical sections. The hook depth variation was traced around the slab perimeter. The maximum hook depth was observed at the corners and concave curvature was observed on a 45 degree vertical section from the corner. Horizontal cross sections through the oscillation marks near the corners provide evidence that liquid steel overflow caused the oscillation mark. Shrinkage of the corner allows the overflowing steel to penetrate deeper into the larger corner gaps, giving rise to oscillation marks that point down in the casting direction at the corner. These results also explain the complex, three-dimensional subsurface microstructures observed near the corners of the slab, and quantify the hook depth and shape.

Keywords: Casting; Solidification microstructure; Ultra-low carbon steel; Continuous Casting

1. Introduction

Deep oscillation marks (OMs)[1] and subsurface hooks[2] in continuously-cast steel slabs are associated with many slab quality problems. Specifically they tend to entrap argon bubbles and alumina inclusions near the hooks[3, 4], leading to slivers and blisters, and transverse cracks often form near the roots of deep OMs[5-7]. In extreme cases, the entire slab surface must be ground or “scarfed” to remove all traces of the hook microstructure, resulting in high cost and loss of productivity[8]. As shown in Figures 1 and 2, OMs are periodic depressions or grooves in the strand surface that run around the perimeter of continuous-cast steel. Subsurface hooks are distinctive micro-structural features which extend from some oscillation marks and can be

identified by etching transverse sections near the slab surface[1, 2, 6]. The curved hook in Figure 1(a) contains a trapped argon bubble.

Hooks and OMs form due to many interdependent, transient phenomena that occur simultaneously during initial solidification near the meniscus. Several different mechanisms have been proposed in previous literature. J. Sengupta et al.[9] have recently suggested a new mechanism for hook and OM formation, that is illustrated in Figure 1(b). Hook formation starts when undercooled liquid steel at the meniscus freezes. Overflow of the solidified meniscus then occurs when the new liquid meniscus becomes unstable, which usually happens at the beginning of the negative strip period[10] during mold oscillation. Dendrites solidify away from the meniscus, which persists in the final microstructure as a distinct "line of hook origin". The extent that the overflowing liquid steel can penetrate into the flux channel determines the final shape of the upper side of the OM.

This mechanism was based on a careful analysis of numerous specially etched samples from ultra-low-carbon steel slabs combined with literature review, previous measurements, observation, and theoretical modeling results[10]. It is supported by microstructural evidence obtained using[9] optical microscopy, scanning electron microscopy (SEM), electron backscattering diffraction (EBSD), energy dispersive X-ray spectroscopy (EDXS), and electron probe micro-analysis (EPMA) techniques. The truncated shape of the curved hook in Figure 1(a) is explained by brittle fracture (hot tearing) of the fragile semi-solid near hook tip during overflow[10]. The fractured hook tip usually melts or is transported away by the flowing liquid steel, but a few micrographs contained a fractured hook tip that was captured nearby, proving this mechanism[9]. The slight microsegregation accompanying dendritic solidification showed that growth proceeded in both directions from the line of hook origin[9]. The line of hook origin

was found to divide regions of different orientation in the steel, even after several phase transformations[9].

Previous understanding of hook and OM formation is based entirely on two-dimensional (2-D) vertical-section micrographs, such as Figure 1(a), which reasonably represent the microstructure around most of the slab perimeter. Near the corners of the slab, however, OMs and hooks exhibit complex 3-D shapes, with different internal microstructures that were unknown before this work.

The present study was conducted to reveal the complex 3-D shape of the frozen meniscus hooks and OMs near the slab corners. Samples of ultra-low carbon steel were studied because these grades (C≤0.05%) are particularly prone to both OM and hook defects. A variety of cross sections near the slab corners were specially etched and analyzed to distinguish the frozen meniscus shape, including vertical, horizontal, and angle sections at different depths and locations in three slab samples taken from the slab corners. The results provide unique evidence of sub-surface micro-structural evolution in the meniscus region near the slab corners of continuous-cast steel.

2. Experimental

Samples from the slab corners of 230 X 1300mm ultra-low carbon steel slabs were obtained from plant experiments performed on #2-1 conventional slab caster at POSCO, Gwangyang Works, South Korea, which features a conventional parallel-mold, standard two-port submerged entry nozzle, non-sinusoidal hydraulic mold oscillator and electromagnetic brake ruler system. The casting speed was kept relatively constant at 1.45m/min. Table 1 summarizes the casting conditions employed during casting of the slabs that contained the samples. The casting conditions of samples I, II, and III match the conditions of Tests 10, 3 and 9 in Ref[11]

respectively. Further details of these plant experiments, including the composition of the ultralow-carbon steel grade and mold powder is given in Ref[11].

Sample I (10mm wide x 20mm deep x 20mm long) encompassed 2 OMs and was obtained near the corner, as shown in Figure 2(a). Horizontal sections were cut through the tip of the oscillation marks at the corner at 0.3mm, 0.8mm, and 1.0mm locations above the OM tip, as shown in Figure 2(b), Optical micrographs are presented for the 1st oscillation mark.

Sample II (13mm wide x 20mm deep x 30mm long) encompassed 4 OMs and was obtained near the corner of a different slab, as shown in Figure 3(a). Vertical sections through this sample were taken at various distances (0.7 to ~5.5mm) from the wide face surface, by polishing, etching, photographing, and then regrinding at intervals of about 0.5mm, as shown in Figure 3(b). These sections parallel to the wide face revealed characteristic subsurface micro-structural features, which were interpreted by extracting hook shapes to construct the 3-D hook shape. Further vertical sections were taken at 20mm, 75mm and 115mm (center line) from the slab corner from the same slab and hook depths and shapes were measured from micrographs of each section.

Sample III (100mm long and encompassing 9 OMs) was obtained near the corner from a different slab and was divided into three pieces each about 30mm long, as shown in Figure 4(a). Each sample was then cut at a different vertical orientation to reveal the subsurface microstructures, as shown in Figure 4(b) through (d).

Further slab samples were taken for other conditions (Heats 4 and 5[8]) and hook depths were measured from vertical sections taken from each sample around the perimeter of the narrow face (5 locations) and wide face (7 locations).

All of the sections were ground, polished, and then etched by a special etching method[10] to reveal the microstructure and hook shapes in ultra-low carbon steel samples. The etching reagent was picric acid solution (2,4,6-trinitrophenol) with additions of surfactant zephiramine (benzyldimethyl-n-tetradecylammonium chloride) and etched for ~1-1.5 h. Further details are given elsewhere[10].

3. Results and discussion

3.1. Overflow mechanism of liquid steel at the corner

Oscillation marks are well known to "point" downwards at the corners, indicating the casting direction, as in Figure 2(a). The lowest point of each oscillation mark is found at the corner, extending 2-3mm below the average around the perimeter, as shown in Figure 3(b). The reason for this is clarified by analysis of the horizontal section micrographs of Sample I in Figures 2 and 5, which also reveal new insights into hook formation in the slab corner.

Each micrograph in Figure 5 exhibits two distinct layers of frozen steel at the corner, which formed at different times. The schematic in Figure 2(b), explains the appearance of these microstructural features. After the 3-D meniscus in the corner freezes to form the hook, it shrinks to pull away from the mold walls. Liquid steel overflows the solidified meniscus, as pictured in Fig. 1(b), and then flows down into the corner gap between the hook and the mold. It can flow further downward in the corner region, owing to the shrinkage gap there. As the overflowing liquid freezes, its horizontal cross section naturally decreases, ultimately ending in a tip, which forms the point of the OM tip at the corner. A small thin layer, which is outlined with a solid red line in Figure 5, is seen on the surface at the corner clearly shows evidence of this phenomenon. The area of this outlined solid red line decreases in size with decreasing vertical distance to the OM point (i.e. from 1.0 to 0.8 to 0.3mm). These areas slice through the base of the hook, which

was originally the frozen meniscus. Furthermore, the enlarged inset in Figure 5(c) clearly shows valleys on each side of this surface layer, which represent the vertical component of the steep-sloping OMs near the corners, observed in Figure 2(a). The distinct microstructure of this layer indicates that it formed later, from liquid running down the surface.

The tip of this overflowed region penetrates further into the corner, where the gap between the mold and the frozen meniscus hook is largest. This larger gap also decreases heat transfer in the corner prior to the overflow, leading to less meniscus freezing. This explains why the hook is thinner in the corner, which is seen by following the hook, demarked by the dark thin discontinuous subsurface line, around the corners in Figure 5.

3.2 Analysis of 3-D subsurface hook shape around the corner

Micrographs of vertical sections (Sample II) presented in Figure 6 show great differences in hook shapes near the corner. The curved line along the center of each hook represents the "line of origin" of the hook, and indicates the shape of the meniscus when it froze. Solidification then proceeded in both directions away from this line, slowing temporarily when thermal gradients diminished, to leave the dark bands that outline each hook. The lines of hook origin traced from a series of ten such vertical sections are shown in Figure 7(a). A true three-dimensional schematic of the hook shape around the slab corner, given in Figure 7(b), was constructed from the hook outlines surrounding the 2nd OM. The upper lines (solid) outline the liquid that overflowed the frozen meniscus. The lower lines (dashed) indicate the boundary between the supercooled frozen meniscus and the molten steel pool below. The vertical distance in Figure 7 is measured in the casting direction relative to the arbitrary zero-reference height taken midway between the first and second oscillation marks.

Figure 8 was constructed to show the top view of the three OM hooks in Figure 7(a). This graph clearly reveals the three-dimensional shape of the frozen meniscus and hooks, which extends continuously from the OM perimeter around the slab corner. The 3rd OM hook is consistently smaller than its neighbors. This indicates that changes in meniscus conditions extending around the corner but lasting less than a second are very common. This is likely due to transient fluid-flow phenomena, such as surface level and superheat fluctuations, which vary even under steady casting conditions. Figure 8 also explains the observation in Figure 6 that the 2nd OM hook is triple the depth of the 3rd OM at 2.5 mm from the corner, but only twice the depth at 3.5mm.

The micrograph in Figure 9(a) shows the deepest extent of the hooks, which is observed in a 45 degree vertical cross section from the corner, as shown in Figure 4(c). Figure 9(b) shows the approximate 2-D hook shape constructed at different vertical sections through different oscillation marks near the corner. The hooks at the corner start about 0.75mm lower than other two nearby observations. This indicates the downward-pointing OM caused by the furthest penetration of overflowing liquid steel into the flux channel at the corners, as discussed earlier. Narrow-face hooks are slightly deeper than wide-face hooks, owing to the generally lower superheat there, and correspondingly more meniscus freezing. This effect is greatly exaggerated in Figure 9 b), due to the proximity of the 2-D sections to the corner. This same reason causes the difference between hook depths in Figure 6, and is explained with Figure 8.

Figure 9(b) also shows that corner hooks at the 45 degree plane sometimes exhibit concave curvature. At other locations, hooks are always convex-shaped, and match well with Bikerman's equation, as observed clearly in previous work[8-11]. This concave curvature at the corner, can not predicted by the two-dimensional equilibrium meniscus shape of Bikerman's equation, which is determined solely by the balance of surface tension and ferrostatic pressure forces [12, 13].

This observation suggests that other effects, such as three-dimensional, transient pressure variations caused by the moving slag rim attached to the mold wall are more influential near the slab corners than elsewhere. This is consistent with a thicker solidified flux rim in the colder corners.

3.3. Hook shape around slab perimeter

Figure 10 compares hook depths around the perimeter of slab sample II, as shown in Figure 3(a). The maximum hook depth appears at the corners, owing to further meniscus solidification, likely due to the colder liquid found in this region. Hook depths[8] measured around the slab perimeter are shown Figure 11. Hooks extend continuously around the entire slab perimeter, although they are often difficult to etch. The hooks are always deepest at the corners, by 10 to 100%. Differences between the inner- and outer-radius widefaces (front and back sides) of the strand are negligible. Hooks are often deeper towards the narrow faces although significant asymmetry is observed between sides.

4. Conclusions

The 3-D shape of the frozen meniscus, subsurface hook microstructure, and oscillation marks in continuous-cast ultra-low carbon steel slabs has been investigated by analyzing micrographs of carefully-etched samples near the corners. The horizontal sections provide clear evidence that OMs formation due to liquid steel overflow. The line of hook origin in the subsurface microstructure indicates the original shape of the frozen meniscus.

A graphical reconstruction of the 3-D hook shape in the corner from a series of vertical cross sections explains the progression of 2-D hook microstructures observed around the slab

perimeter. The classic 2-D hook microstructure simply curves continuously around the corner, increasing in size towards the corner. The shape, size, and depth of this continuous hook structure have been quantified.

The 3-D shape of the continuous plane of hook origin matches the expected shape of the frozen meniscus in the corner. Deeper hooks in this region might arise from lower superheat, or higher pressure from the deeper flux rim during mold oscillation expected in the corner. These results confirm the mechanism for the formation of hooks and OMs by meniscus solidification and subsequent liquid steel overflow suggested by J. Sengupta et al.[9] Oscillation marks extend further in the casting direction at the corner due to the ease of liquid steel overflow into the larger gap there. These results will provide a foundation for future computational models and plant trials to understand and control hook and OM formation near the slab corners.

ACKNOWLEDGEMENTS

Financial support from the Korea Research Foundation Grant funded by the Korean Government (MOEHRD), (KRF-2005-213-D00110), the Continuous Casting Consortium at the University of Illinois at Urban-Champaign, and the National Science Foundation (Grant DMI 04-23794) is acknowledged for support this project. The authors also thank Dr. J. Sengupta for providing initial help and POSCO, Gwangyang Works, S. Korea for providing the samples.

REFERENCES

1. Takeuchi, E., J.K. Brimacombe. The formation of oscillation marks in the continuous casting of steel slabs. Met. Trans B 1984;15B(Sept):493-509.
2. Emi, T., H. Nakato, Y. Iida, K. Emoto, R. Tachibana, T. Imai, H. Bada. Influence of physical and chemical properties of mold powders on the solidification and occurrence of surface defects of strand cast slabs. Proceedings of National Open Hearth and Basic Oxygen Steel Conference 1978;61:350-361.

3. Schmidt, K.D., F. Friedel, K. Imlau, W. Jager, K.T. Muller. Consequent improvement of surface quality by systematic analysis of slabs. Steel Research International 2003;74(11-12):659-666.
4. Birat, J., M. Larrecq, J. Lamant, J. Petegnief. The Continuous Casting Mold: A Basic Tool for Surface Quality and Strand Produtivity. In: Mold Operation for Quality and Productivity, A.W. Cramb, E. Szekeres, editors., Iron and Steel Society, Warrendale, PA, 1991. p. 3-14.
5. Brimacombe, J.K., K. Sorimachi. Crack Formation in the Continuous Casting of Steel. Metall. Trans. B 1977;8B:489-505.
6. Takeuchi, E., J.K. Brimacombe. Effect of Oscillation-Mark Formation on the Surface Quality of Continuously cast Steel Slabs. Met. Trans B 1985;16B(Sept):605-625.
7. Harada, S., S. Tanaka, H. Misumi, S. Mizoguchi, J. Horiguchi. A formation mechanism of transverse cracks on CC slab surface. ISIJ International 1990;30(4):310-316.
8. Shin, H.-J., B.G. Thomas, G.G. Lee, J.M. Park, C.H. Lee, S.H. Kim. Analysis of Hook Formation Mechanism in Ultra Low Carbon Steel using CON1D Heat Flow - Solidification Model. Materials Science & Technology 2004; New Orleans, LA: TMS, Warrendale, PA, 2004;II. p. 11-26.
9. Sengupta, J., H.-J. Shin, B. G. Thomas, S.-H. Kim. Micrograph Evidence of Meniscus Solidification and Sub-Surface Microstructure Evolution in Continuous-Cast Ultra-Low Carbon Steels. Acta Materialia 2006;54(4):1165-1173.
10. Sengupta, J., B.G. Thomas, H.J. Shin, G.G. Lee, S.H. Kim. Mechanism of Hook Formation during Continuous Casting of Ultra-low Carbon Steel Slabs. Metallurgical and Materials Transactions A 2006;37A(5):1597-1611.
11. Shin, H.-J., G.G. Lee, W.Y. Choi, S.M. Kang, J.H. Park, S.H. Kim, B.G. Thomas. Effect of Mold Oscillation on Powder Consumption and Hook Formation in Ultra Low Carbon Steel Slabs. AISTech 2004; Nashville, TN: Assoc. Iron Steel Technology, 2004. p.
12. Bikerman, J.J. Physical Surfaces: Academic Press, Inc., New York, 1970.
13. Fredriksson, H., J. Elfsberg. Thoughts about the initial solidification process during continuous casting of steel. Scandinavian Journal of Metallurgy 2002;31:292-297.

.

Table 1 - Casting conditions for slab samples

Sample number	Pour temperature (˚C)	Mold oscillation stroke (mm)	Mold oscillation frequency (cpm)	Non-sinusoidal mold oscillation ratio (%)	Superheat (˚C)
Sample I	1559	7	145	12	26
Sample II	1571	5	174	12	30
Sample III	1559	7	124	0	26

Note) Samples I, II and III were taken during tests 3, 9 and 10, respectively in Ref[12].

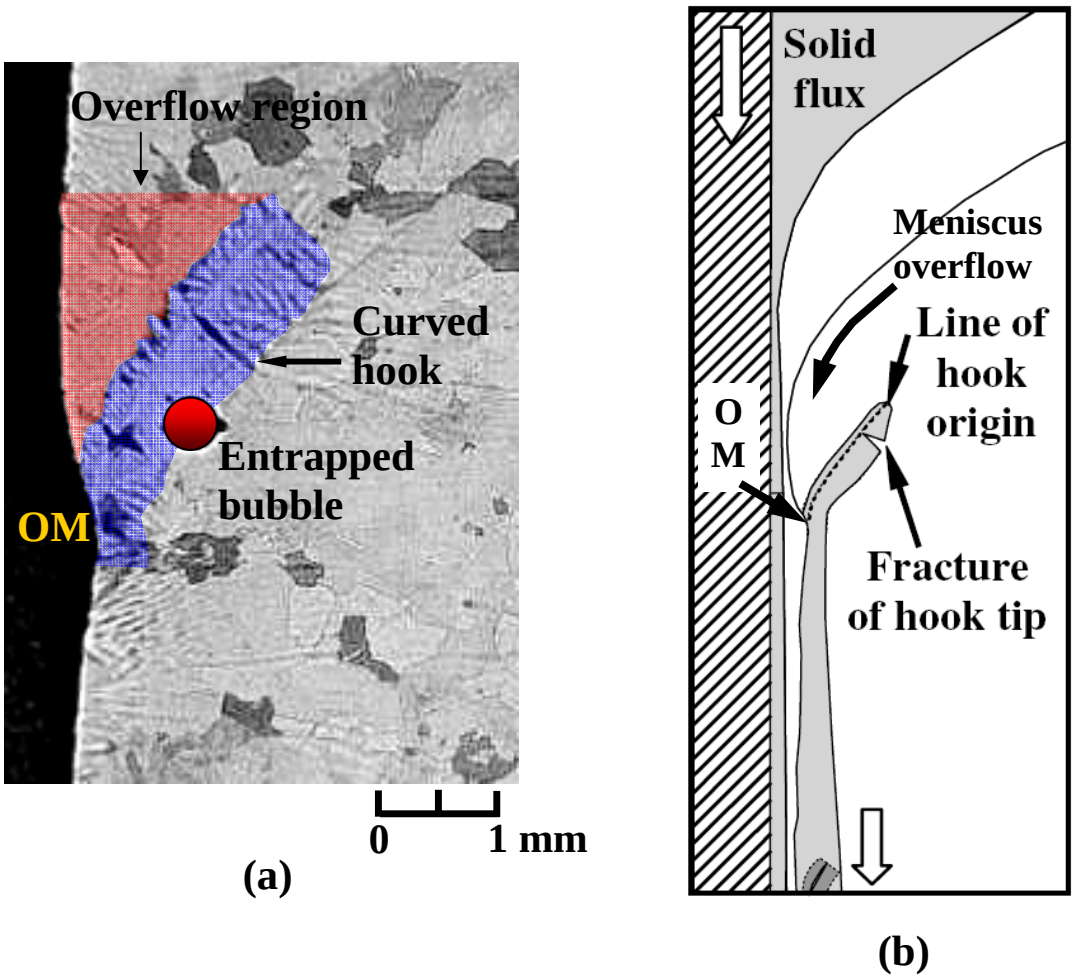

Figure 1 – Optical micrograph(a) of an ultralow-carbon steel sample showing entrapment of argon bubble by a curved hook-type oscillation mark and (b) schematic illustrating formation of curved hooks by meniscus solidification and subsequent liquid steel overflow[10].

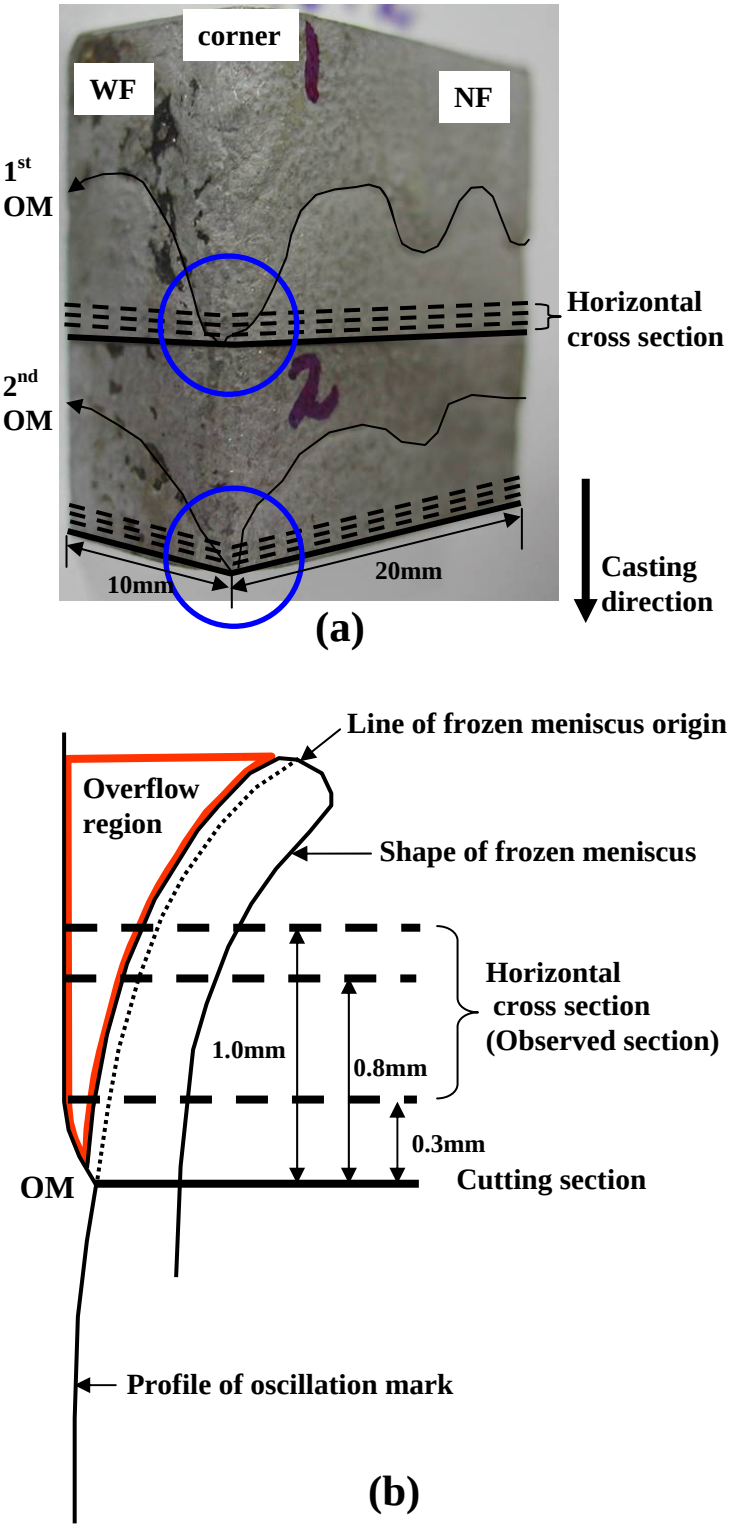

Figure 2 – Sample I (a) location obtained from slab corner and (b) three different horizontal sections cut for microscopy analysis of hooks and oscillation mark shown in circles.

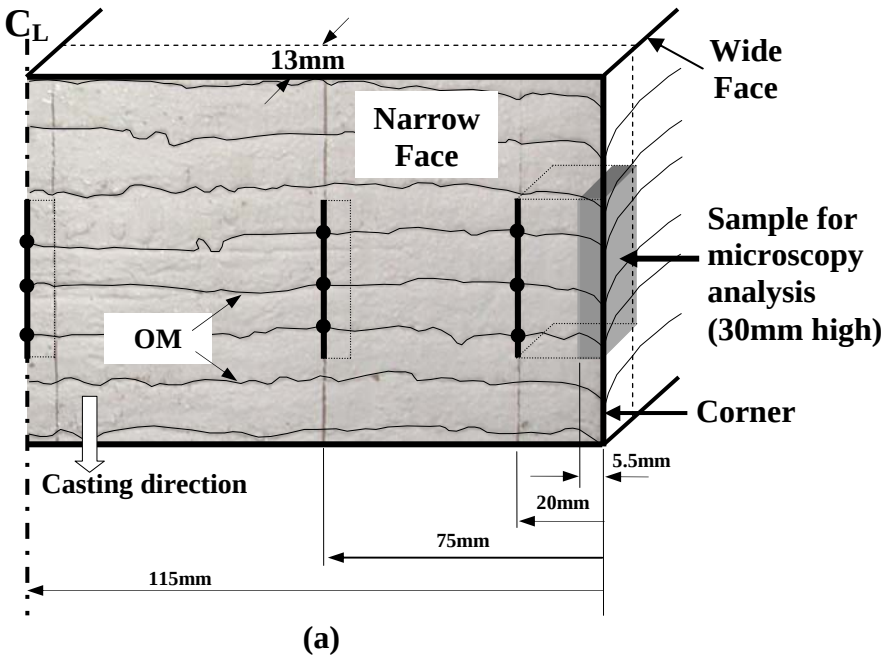

(a)

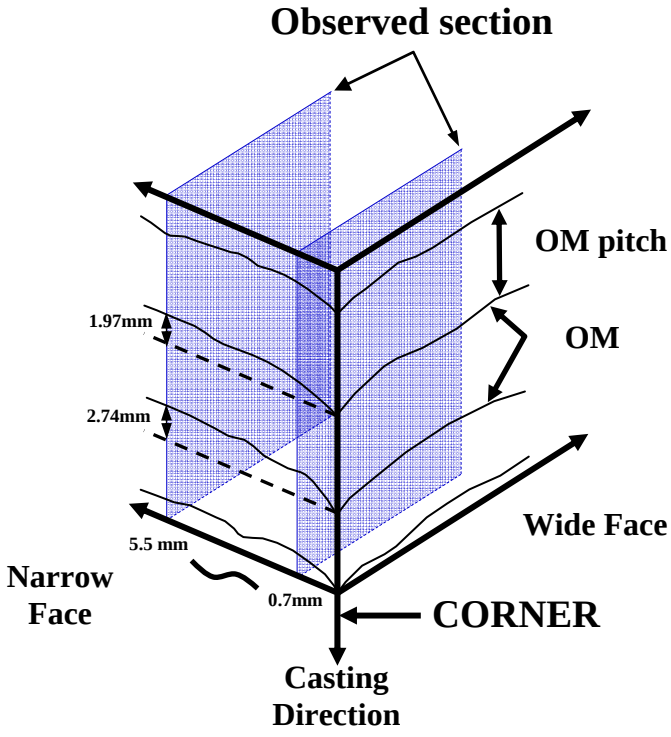

(b)

Figure 3 – Sample II (a) location obtained from slab corners and (b) location of sections cut for microscopy analysis showing oscillation mark shape.

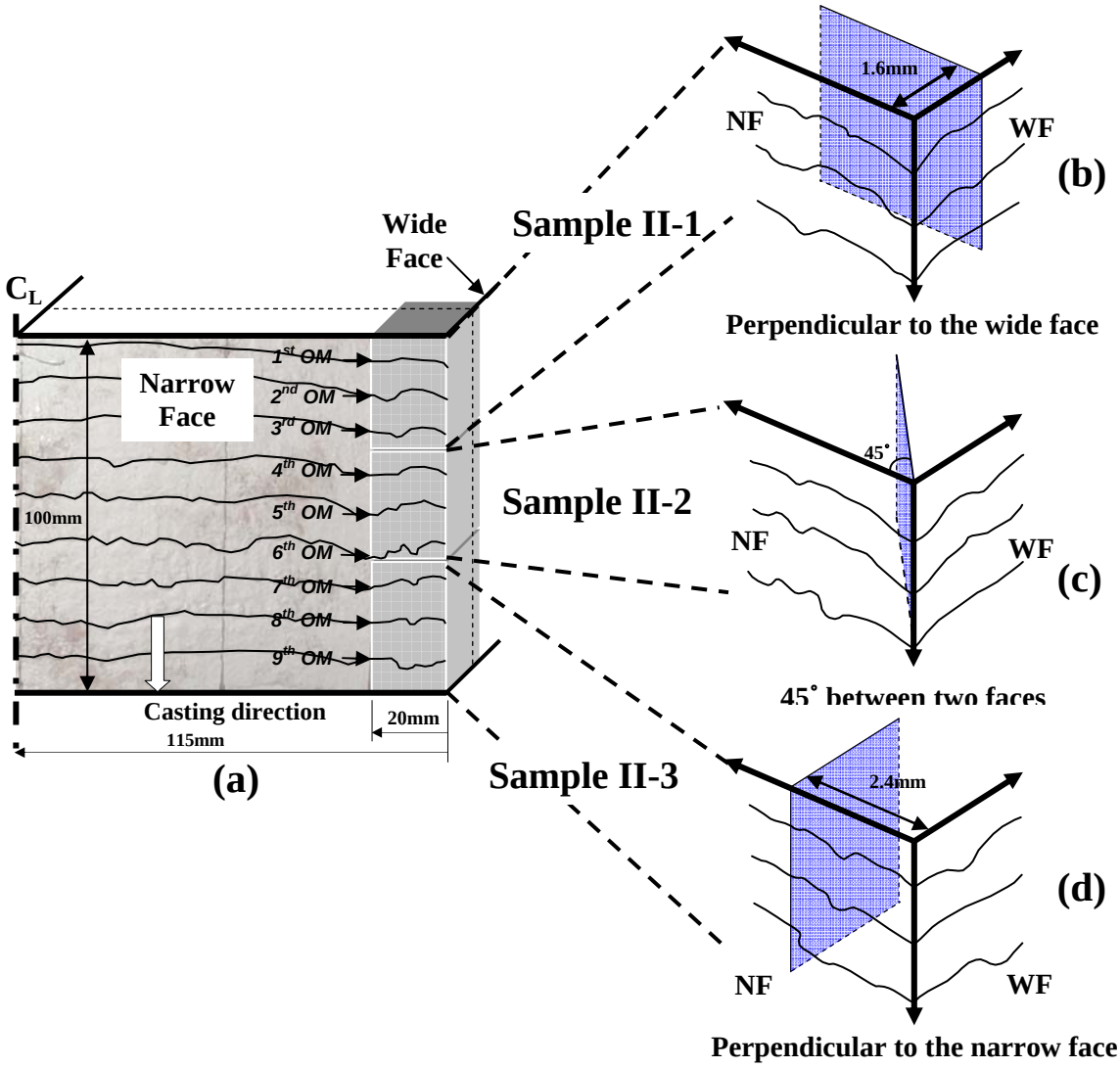

Figure 4 – Sample III (a) location obtained from slab corners and (b)~(d) orientation of three different vertical sections cut for microscopy analysis.

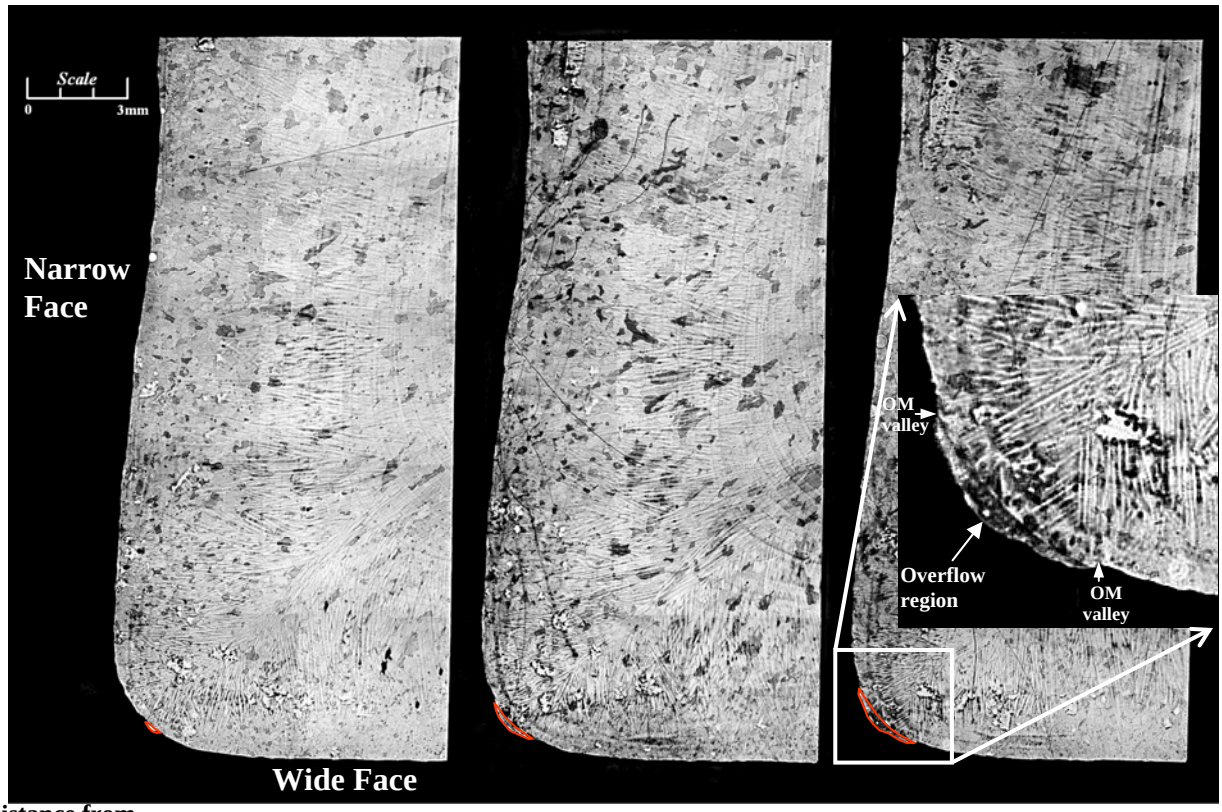

Figure 5 – Optical micrographs of horizontal cross sections (Sample I) showing evidence of liquid steel overflow.

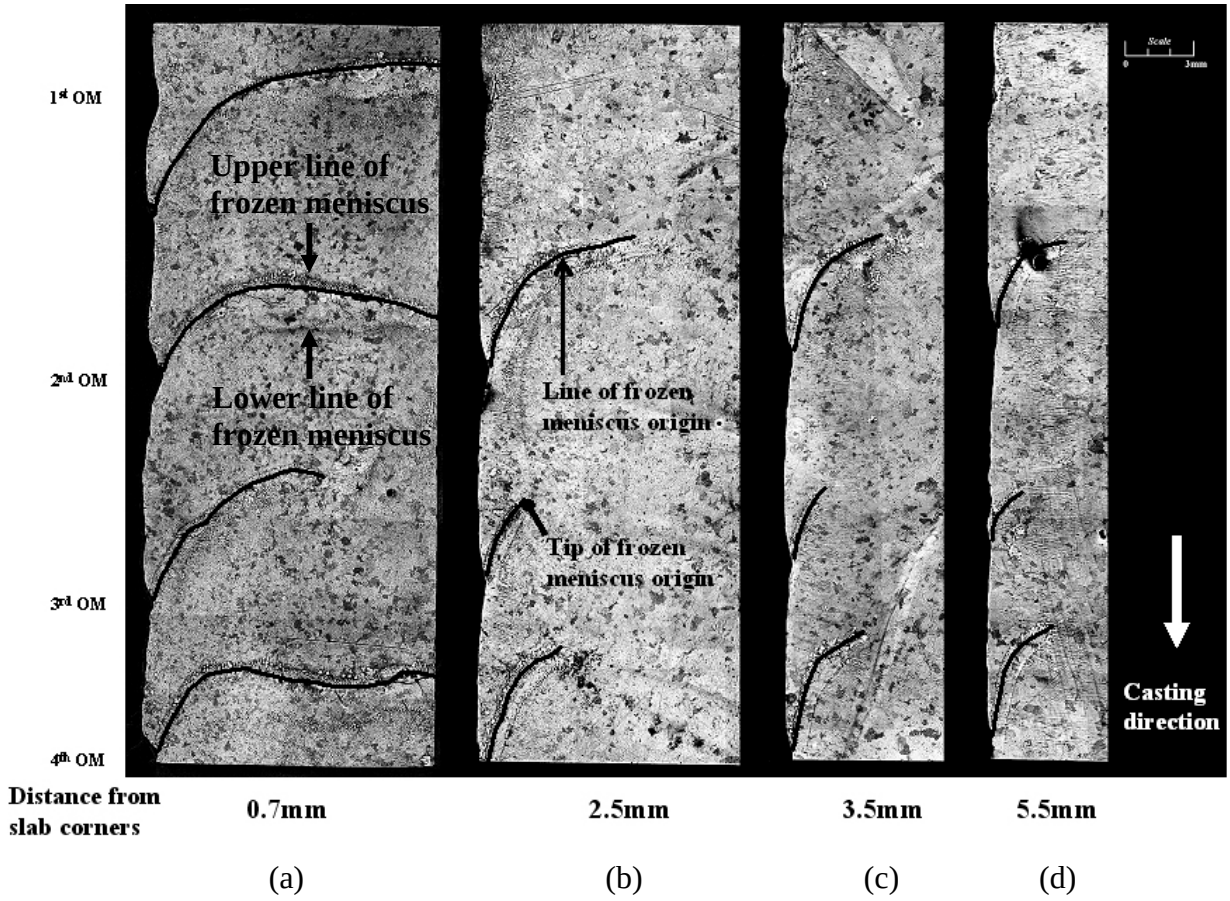

Figure 6 – Optical micrographs at different distances from wide face (sample II) showing line of frozen meniscus origin: “hooks”.

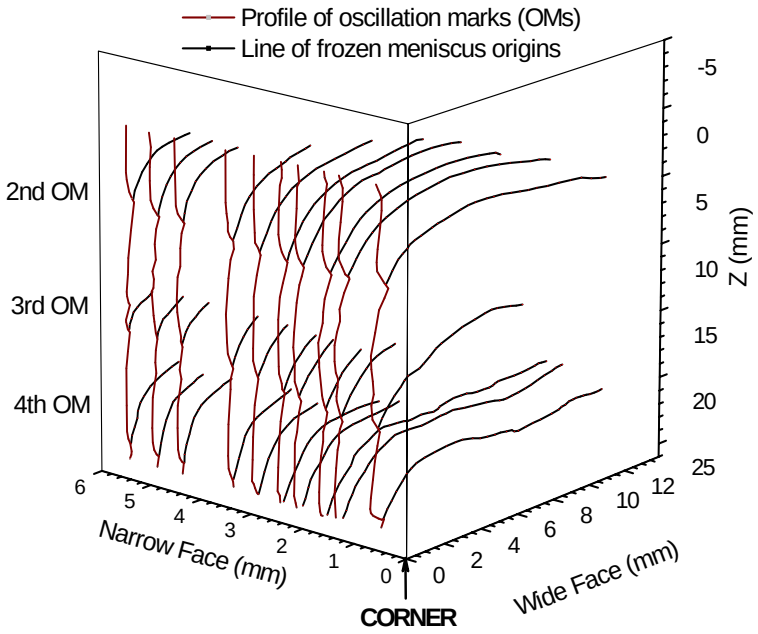

(a)

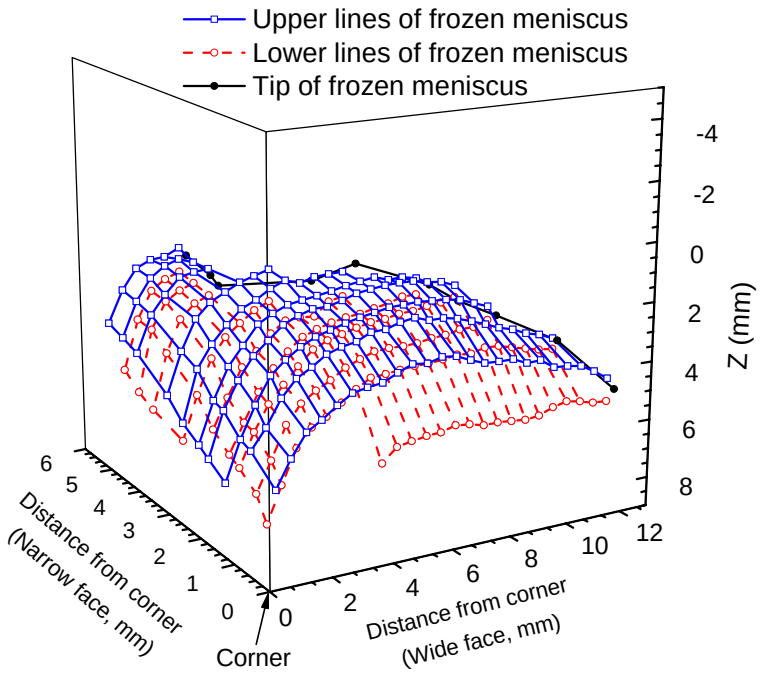

(b)

Figure 7 – Line of frozen meniscus origins obtained from micrograph analysis of Sample II (a) and (b) 3-D shape of frozen meniscus hook at 2nd OM

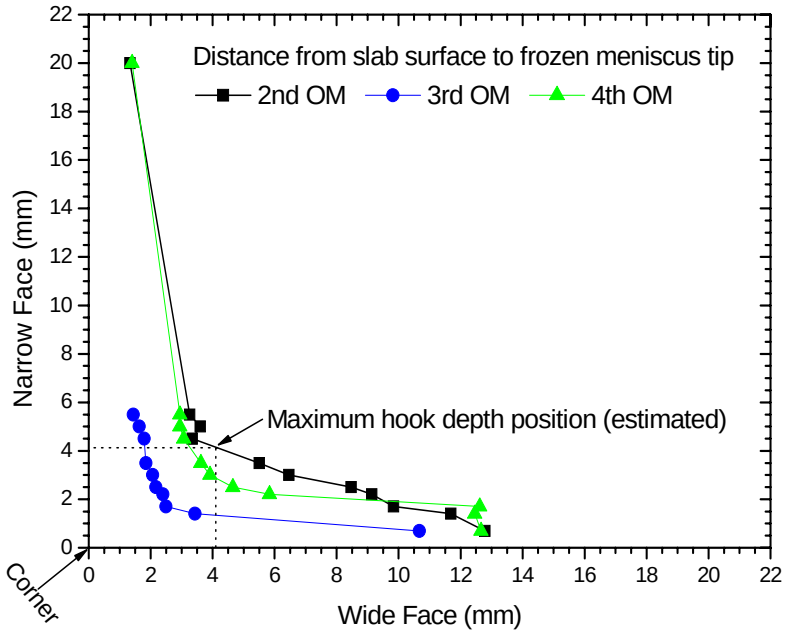

Figure 8 – Top views of lines of frozen meniscus origins (hooks) from micrographs (Sample II) showing hook depth increase around corner and explanation of hook depth variations observed in micrographs.

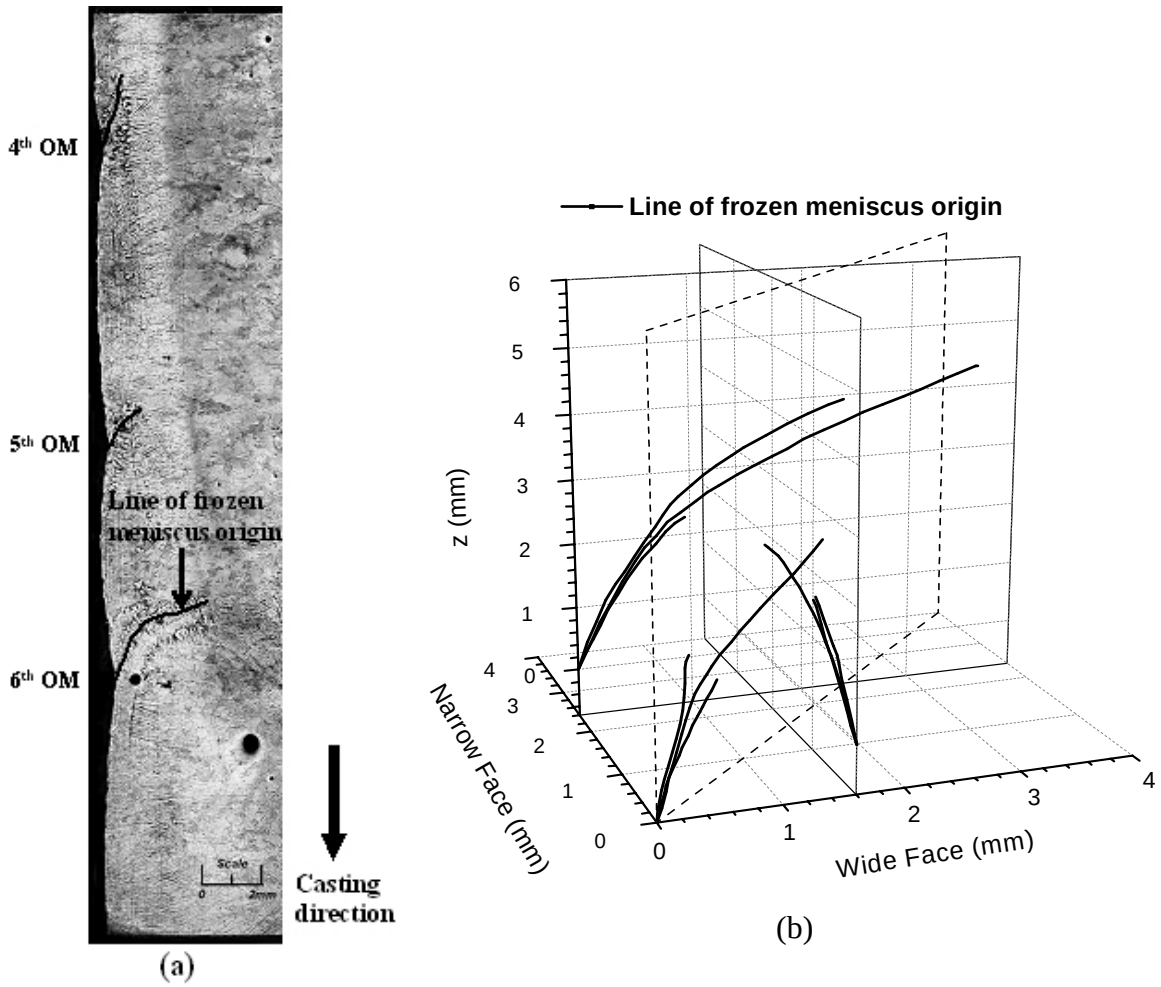

Figure 9 – Hook shapes (lines of frozen meniscus from vertical sections through sample III) (a) micrograph of 45 degree section and (b) shapes traced from three different hooks.

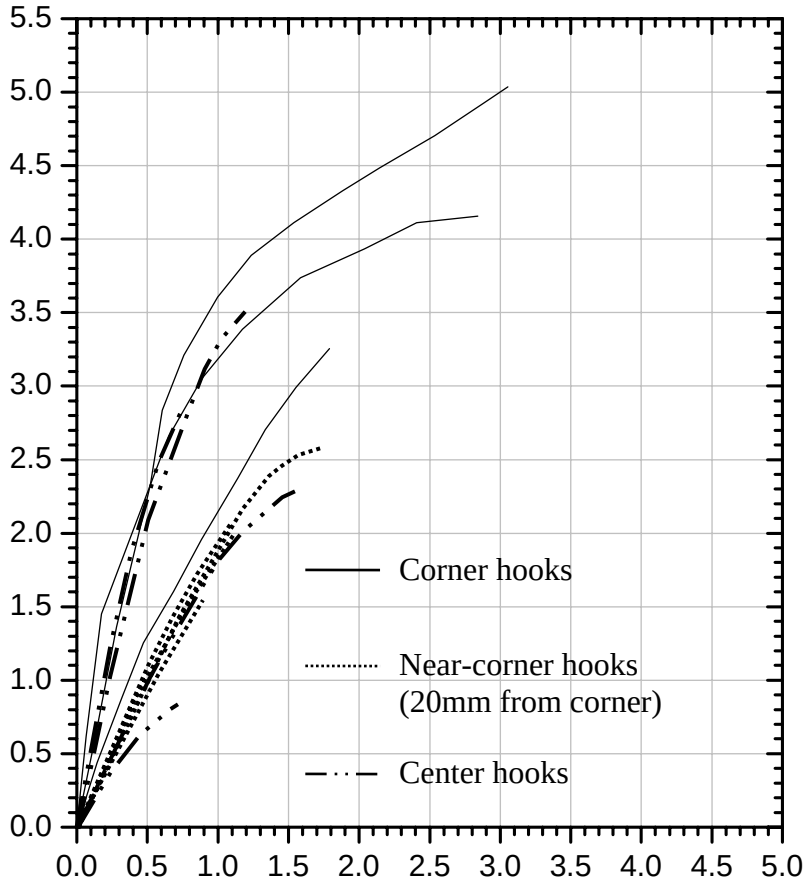

Figure 10 – Lines of frozen meniscus (sample II) at three locations along the narrow face, showing increase in hook size towards corner

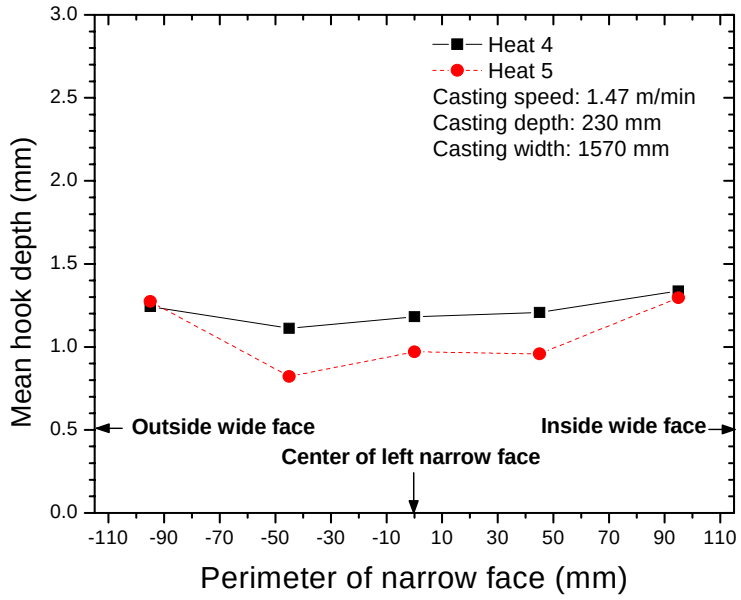

(a)

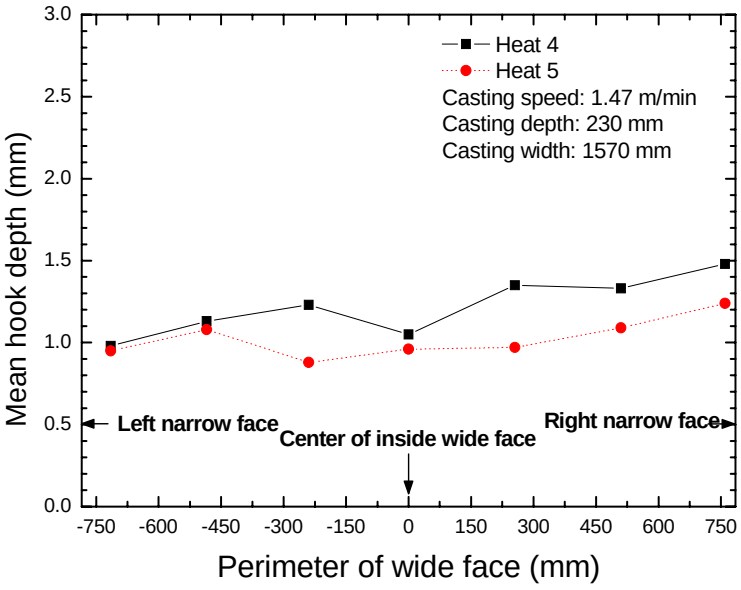

(b)

Figure 11 – Hook depth variation along mold perimeter of (a) narrow face and (b) wide face